Modulation of the Midpoint Potential of the [2Fe−2S] Rieske Iron Sulfur Center by Q_o Occupants in the bc_1 Complex†

Vladimir P. Shinkarev,* Derrick R. J. Kolling, Tim J. Miller, and Antony R. Crofts*

Department of Biochemistry, University of Illinois at Urbana-Champaign, 156 Davenport Hall, 607 South Mathews Avenue, Urbana, Illinois 61801

Received May 28, 2002; Revised Manuscript Received October 2, 2002

ABSTRACT: Following addition of myxothiazol to antimycin-treated chromatophores from *Rhodobacter sphaeroides* poised at an ambient redox potential (E_h) of ∼300 mV, the amplitude of the flash-induced cytochrome c_1 oxidation in the ms range increased, indicating a decrease in the availability of electrons from the immediate donor to c_1, the Rieske iron−sulfur protein (ISP). Because the effect was seen only over the limited E_h range, we conclude that it is due to a decrease in the apparent midpoint redox potential (E_m) of the ISP by about 40 mV on addition of myxothiazol. This is in line with the change in E_m previously seen in direct redox titrations. Our results show that the reduced ISP binds with quinone at the Q_o site with a higher affinity than does the oxidized ISP. The displacement of ubiquinone by myxothiazol leads to elimination of this preferential binding of the ISP reduced form and results in a shift in the midpoint potential of ISP to a more negative value. A simple hypothesis to explain this effect is that myxothiazol prevents formation of hydrogen bond of ubiquinone with the reduced ISP. We conclude that all Q_o site occupants (ubiquinone, UHDBT, stigmatellin) that form hydrogen bonds with the reduced ISP shift the apparent E_m of the ISP in the same direction to more positive values. Inhibitors that bind in the domain of the Q_o site proximal to heme b_L (myxothiazol, MOA−stilbene) and displace ubiquinone from the site cause a decrease in E_m of ISP. We present a new formalism for treatment of the relation between E_m change and the binding constants involved, which simplifies analysis. Using this formalism, we estimated that binding free energies for hydrogen bond formation with the Q_o site occupant, range from the largest value of ∼23 kJ mol^{-1} in the presence of stigmatellin (appropriate for the buried hydrogen bond shown by structures), to a value of ∼3.5 kJ mol^{-1} in the native complex. We discuss this range of values in the context of a model in which the native structure constrains the interaction of ISP with the Q_o site occupant so as to favor dissociation and the faster kinetics of unbinding necessary for rapid turnover.

The cytochrome bc_1 complex (ubiquinol: cytochrome *c* oxidoreductase and related complexes) plays a central role in free-energy transduction in all major electron-transfer chains (reviewed in ref *1*). The functional core of the complex consists of 3 catalytic subunits that contain four redox centers (two cytochrome *b* hemes, cytochrome c_1, and an iron−sulfur center, ISP[1]) and two quinone-processing sites, for oxidation of ubiquinol (Q_o site) and reduction of ubiquinone (Q_i site). In the bc_1 complex from *Rhodobacter sphaeroides*, two *b*-type hemes, b_L and b_H, have redox midpoint potentials (E_m) of −90 and 50 mV, respectively. Cytochrome c_1 ($E_{m,7} \approx$ 260 mV) and the Rieske iron−sulfur protein (ISP) ($E_{m,7} \approx$ 300 mV) are the high-potential components of this complex. According to the modified Q cycle (*2*, *3*; reviewed in ref *1*), one electron released upon quinol oxidation at the Q_o site is transferred via the Rieske iron−sulfur protein (ISP) to cytochrome c_1, while the second electron crosses the membrane via a chain of two hemes present in the cyt *b* subunit and reduces the occupant of the Q_i site.

Specific inhibitors have provided valuable tools for the elucidation of structure and function of the bc_1 complexes. Over the years, different inhibitors, specific for each quinone-processing site, have been identified and studied (*4*). Inhibitors of the Q_o site fall into two main classes, initially exemplified by UHDBT and myxothiazol (*5*, *6*). They have been subdivided into two or three types, called either class I and class II (*7*), or Q_o-II and Q_o-III, and Q_o-I (*4*, *8*), based on their different effects on the spectra and redox potentials of heme b_L or ISP and their effects on the kinetics of cyt c oxidation.

Previous work had shown that class II (Q_o-I) inhibitors (myxothiazol and MOA-type inhibitors) occupy a domain of the Q_o site near heme b_L and induce shifts in the spectrum of this heme. They displace more weakly binding inhibitors of either class and all quinone occupants. In the presence of myxothiazol, interactions of the reduced ISP (ISP^{red}) with

† This work was supported by grants from the NIH (GM 53508, GM35438) and USDA (AG 98-35306-7009).

* Corresponding authors. Phone: (217) 333-8725. Fax: (217) 244-6615. E-mails: vshinkar@uiuc.edu and a-crofts@uiuc.edu.

[1] Abbreviations: CCCP, carbonyl cyanide *m*-chlorophenylhydrazone; cyt, cytochrome; DAD, 2,3,5,6-tetramethyl-*p*-phenylenediamine, DMSO, dimethyl sulfoxide; ISP, Rieske iron−sulfur protein; PES, *N*-ethylphenazonium ethosulfate; PMS, *N*-methylphenazonium methosulfate; *Rb.*, *Rhodobacter*; RC, photosynthetic reaction center; UHDBT, 5-undecyl-6-hydroxy-4,7-dioxobenzothiazol; b_L and b_H, low- and high-potential hemes of cytochrome *b*, respectively; E_h, ambient redox potential; E_m, midpoint redox potential; Q, QH_2, oxidized and reduced forms of ubiquinone; Q_i site (Q_o site), quinone reducing (quinol oxidizing) site of bc_1 complex.

10.1021/bi026198c CCC: $22.00
Published on Web 11/08/2002

quinone leading to a prominent $g_x = 1.80$ line are lost. Earlier reports had suggested that the class II inhibitors (in contrast to those of class I) do not change the E_m of ISP significantly (*4*, *8*, *9*). However, there have been indications that class II inhibitors could modify the midpoint potentials of ISP. For example, anomalies in cyt c_{tot} oxidation kinetics following flash activation of *Rb. sphaeroides* chromatophores in the presence and absence of myxothiazol were noted (interpreted as a change in the E_m value of c_1, *10*, *11*), and the binding of MOA−stilbene at the Q_o site was decreased after reduction of the iron−sulfur center and cyt c_1 (*12*), indicating that MOA−stilbene binding at Q_o site can, in turn, modify the midpoint potential of ISP. More recently, Darrouzet et al. (*13*) and Sharp et al. (*14*) noted that myxothiazol and MOA−stilbene, respectively, decreased the midpoint potential of ISP by about 30−50 mV, and the latter group also reported a similar change induced by alcohols (*15*). Darrouzet et al. (*13*, *16*) showed that in mutant strains of *Rb. capsulatus* with changes in length of the linker region joining the extrinsic ISP domain to its anchoring N-terminal section, myxothiazol induced a substantial change in E_m of ISP, from the abnormally high values reported in the absence of inhibitors to values essentially the same as in the wild-type complex in the presence of myxothiazol. All these effects were attributed to differential interaction of the added reagents or the protein with the ISP in oxidized and reduced forms.

Inhibitors of class I (UHDBT as Q_o-II and stigmatellin as Q_o-III) disrupt the electron transfer from ISP to c_1 by a stronger interaction, leading to a change in EPR line shape and an increase in the midpoint potential due to preferential binding to the reduced form of ISP (ISP^{red}) (*4*, *5*, *17*). In line with this, it was found that the binding of stigmatellin to the bc_1 complex depleted of the iron−sulfur protein was almost absent (*18*).

Recent structures for the bc_1 complex from several sources, solved with and without different inhibitors bound at the Q_o site (*7*, *19*−*22*), have revealed the structural basis of the differential properties of the two classes of inhibitors. The Q_o site is a relatively spacious pocket with a binding site for myxothiazol (or similar MOA-inhibitors) close to heme b_L (proximal domain) and a binding site for stigmatellin or UHDBT, distal from heme b_L, that communicates with an interface at which the ISP docks, allowing formation of a hydrogen bond (H-bond) between them. A second feature seen in the structures, and intimately linked to the nature of the Q_o site occupant, was the location of the extrinsic head of ISP in different positions, leading to the suggestion that ISP must function via movement of the catalytic domain (*20*, *21*). When closest to cyt c_1, the distance between the nearest Fe of the [2Fe−2S] cluster and the cyt c_1 heme-Fe is approximately 15 Å (*21*, *22*), which allows for fast electron transfer between them. Binding of UHDBT or stigmatellin leads to displacement of the ISP extrinsic domain to a close docking at an interface with the Q_o site on the surface of cyt *b* that is stabilized by a H-bond. For the stigmatellin structures, this H-bond is between the $N_\epsilon H$ of one of the liganding histidines (His-161 using the residue numbering from the chicken or beef structures) and a carbonyl group of the inhibitor (reviewed in ref *1*). It has been suggested that a similar bond might be involved in a complex with ubiquinone that gives rise to an EPR line at $g_x = 1.80$ in the ISP^{red} spectrum (*7*, *23*, *24*). Binding of class II (Q_o-I) inhibitors led to movement of the extrinsic head to the ISP_C position, loss of contact with the cyt b interface, and loss of the interaction with occupants (*20*, *32*).

In this paper we report that addition of myxothiazol to chromatophores at ambient redox potentials (E_h) in the range ~300 mV led to an increase in the flash-induced oxidation of cyt c_1. Under otherwise similar conditions, addition of myxothiazol to chromatophores at $E_h < 200$ mV, or $E_h > 350$ mV, did not cause an increase in the flash-induced oxidation of cyt c_1. We conclude that this effect of myxothiazol is due to the small decrease of the midpoint potential of ISP when a quinone molecule at the Q_o site is displaced by myxothiazol. We develop a new formalism for analysis of the binding constants involved, propose a new hypothesis to account for the E_m change, and discuss the mechanistic implications.

MATERIALS AND METHODS

Growth of Cells and Isolation of Chromatophores. Cells of the wild-type *Rhodobacter sphaeroides* Ga were grown photosynthetically at 30 °C in Sistrom's medium. Cells of the pC2P404.1 strain (native cyt c_2 superproducer) of *Rb. sphaeroides* Ga (*25*) were grown photosynthetically at 30 °C in Sistrom's medium in the presence of 2 μg/mL tetracycline using far-red filters to minimize antibiotic photooxidation. The cyt c_2 superproducer strain was used in some experiments to minimize delays in transfer of an oxidizing equivalent from RC to the bc_1 complex due to recycling of cyt c_2. Cells of the *BC17C* strain of *Rb. sphaeroides* Ga with His-tagged bc_1 complex expressed in a plasmid (*26*) were grown photosynthetically in Sistrom's medium, in the presence of kanamycin (20 μg/mL) and tetracycline (1.5 μg/ mL) using far-red filters. When grown in the presence of excess tetracycline, His-tagged *BC17C* strains overexpressed the bc_1 complex, so as to yield chromatophores having a higher relative stoichiometry of cytochrome bc_1 complex to RCs compared to the parent Ga strain. Chromatophores were isolated by differential centrifugation as described elsewhere (*27*).

Spectrophotometric Determination of Redox Changes of Cytochromes and Reaction Center. Kinetics of cytochrome redox changes were measured with a single-beam kinetic spectrophotometer of local design. Actinic light pulses were provided by a xenon flash (~5 μs half-duration) or by a frequency-tripled (λ, 355 nm), Q-switched (FWHM, 10 ns) Nd:YAG laser (Surelite II, Continuum, USA) at a flash energy of 160 mJ fed into an optical parametric oscillator (OPO) tuned to 800 nm (output flash energy 12 mJ). Fast flash-induced cytochrome c_2 oxidation kinetics were measured with cooled large area (5 mm in diameter) avalanche photodiode (APD) from Advanced Photonix (Camarillo, USA).

The ambient redox potential in the cuvette was adjusted by adding small amounts of $K_3Fe(CN)_6$ or $Na_2S_2O_4$, and the suspension was kept anaerobic by a constant flow of argon gas above the sample. The following buffer, buffer A, was used in all experiments: 50 mM MOPS (pH 7.0), 100 mM KCl, 1 mM Fe EDTA (redox buffer, $E_m = 117$ mV, *34*), and 1 mM NaCN. The redox changes of cyt c_1 plus cyt c_2 ($= c_{tot}$) were measured at 551−542 nm (ϵ^{mM} ~20 $mM^{-1}cm^{-1}$, *10*, *28*). Cytochrome b_H reduction was measured at 561−

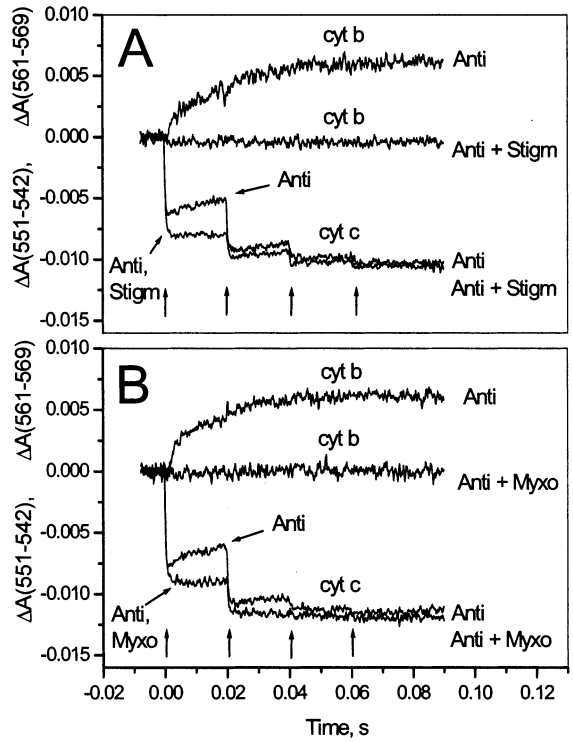

FIGURE 1: The effect of stigmatellin and myxothiazol on the kinetics of flash-induced changes of cytochrome c_{tot} and cytochrome *b* in *Rb. sphaeroides* chromatophores. Chromatophores from His-tagged *BC17C* cells were suspended in buffer A with, in addition, 50 μM DAD (E_m = 245 mV), 50 μM *p*-benzoquinone (E_m = 280 mV), 2 μM PMS (E_m = 80 mV), 50 μM ferrocene (E_m = 420 mV), and 2 mM potassium ferrocyanide (E_m = 430 mV). The concentrations of antimycin A and myxothiazol (both in DMSO solutions) were (when indicated) 7 μM. The concentration of stigmatellin (added as alcohol solution) was 6 μM. The concentrations for CCCP and gramicidin were 2 and 6 μM, respectively. Traces shown are the average of 16 with 20 s between measurements. Redox potential was 265 (panel A) and 280 mV (panel B). Time constant of measurements was 35 μs.

569 nm (ϵ^{mM} ~20 mM^{-1} cm^{-1}, *3*) in the presence of antimycin. The RC concentration was estimated at 542 nm (ϵ^{mM} ~10 mM^{-1} cm^{-1}, *29*).

To minimize interference from overlapping absorbance changes, we also determined the kinetics of c_1 and c_2 from kinetic traces measured at 2−4 nm steps over the wavelength range from 540 to 575 nm, using published spectra for c_2, c_1, P870, b_L, and b_H (*11*). The least-squares method used was similar to that described in Shinkarev et al. (*30*).

Reagents. Antimycin A, CCCP, DAD, myxothiazol, nigericin, DMSO, MOPS, PMS, and valinomycin were obtained from Sigma Chemical Co. Inhibitors and uncouplers were dissolved in ethanol or DMSO and stored at −20 °C.

RESULTS

Effect of myxothiazol on the flash-induced kinetics of cyt c_{tot} at E_h= 300 mV. At ambient redox potential E_h ~ 300 mV, hemes b_L (E_{m7} = −90 mV) and b_H (E_{m7} = 50 mV), and the ubiquinone pool (E_{m7} = 90 mV) are oxidized, and cyt c_1 (E_{m7} = 260 mV) is ~80% oxidized. Flash activation of the RC under these conditions leads to the generation of oxidized cyt c_2 and QH_2, which are the substrates for the bc_1 complex, allowing stoichiometric turnover. Figure 1 shows the flash-induced kinetics of cyt c_{tot} (c_1 + c_2) in *Rb. sphaeroides* chromatophores in the presence of antimycin A, an inhibitor of the Q_i site, and either stigmatellin (panel A) or myxothiazol (panel B) as an inhibitor of the Q_o site. Addition of either stigmatellin or myxothiazol increased the amount of cyt c_{tot} oxidized after the flash and completely blocked the reduction of b_H heme. The stimulation of oxidation by class I (Q_o-II) type inhibitors is well understood from their binding of the ISP^{red} form (*5*). However, since myxothiazol and stigmatellin have very different mechanisms of action, especially with respect to their interaction with ISP, the similarity of their kinetic effect here seems to be paradoxical.

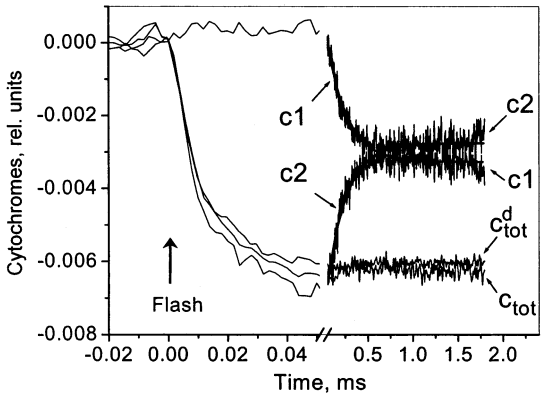

FIGURE 2: The kinetics of flash-induced changes of cytochromes c_1, c_2, and c_{tot} in *Rb. sphaeroides* chromatophores (pC2P404.1 strain). The kinetics of c_1 and c_2 were obtained by deconvolution of absorbance changes measured over the wavelength range from 540 to 560. Cytochrome c^d_{tot} is obtained as sum of cytochromes, c_1 + c_2, restored from deconvolution. Cytochrome c_{tot} was measured as the difference between absorbance changes at 551 and 542 nm. Chromatophores were suspended in buffer A plus 50 μM DAD, 10 μM valinomycin, 10 μM nigericin, 0.5 mM sodium ascorbate. Traces shown are the average of 32, with 10 s between measurements. Time constant of measurements was 1.7 μs.

Spectral Deconvolution of c_1 and c_2. To understand the separate contributions of c_1 and c_2 to the observed effect of myxothiazol, we extracted the kinetics from traces measured over the wavelength range from 540 to 560 nm, using the least-squares method and spectra of individual cytochromes (*31*). In comparison to the traditional method based on measurements using wavelength pairs (550−554 nm for c_2 and 552−548 nm for c_1, *10*), this allows a more precise assignment of changes to cyt c_2 or c_1.

Figure 2 shows the laser-induced kinetics of c_1 and c_2 obtained from such a deconvolution of the kinetics measured on a relatively fast time scale. The c_1 is oxidized after a short delay (~50 μs, Figure 2), reflecting the time needed for c_2 to be oxidized by $P870^+$ and to diffuse to the bc_1 complex. The kinetics of further oxidation of c_1 coincide well with kinetics of cyt c_2 reduction, with a halftime of ~200 μs. The sum of c_1 + c_2 restored from deconvolution, c^d_{tot} = c_1 + c_2 is practically identical to normalized c_{tot} measured at 551−542 nm. This indicates good consistency of our deconvolution and traditional measurements based on the use of a pair of wavelengths for c_{tot}. From the results presented in Figure 2, we conclude that our procedure gives reliable results for separation of the flash-induced kinetics of cytochromes c_1 and c_2.

Effect of Myxothiazol on Flash-Induced Kinetics of Cytochromes c_1 and c_2 at 300 mV. Figure 3 shows the effect

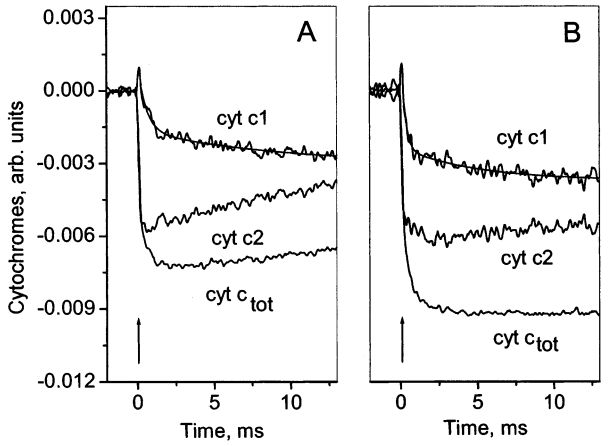

FIGURE 3: The kinetics of cytochrome changes in the presence of antimycin alone (A) and in the presence of both antimycin and myxothiazol (B) in wild-type *Rb. sphaeroides* Ga chromatophores. Chromatophores were suspended in buffer A plus 100 μM DAD, 2 μM PMS, 2 μM PES (E_m = 55 mV), and 2 mM potassium ferrocyanide. The redox potential was poised at 286 mV. The concentration of antimycin A was 6 μM. Traces shown are the average of 16, with 20 s (in the presence of antimycin alone) or 45 s (in the presence of both antimycin and myxothiazol) between measurements. The concentration of myxothiazol was 6 μM. Time constant was 35 μs.

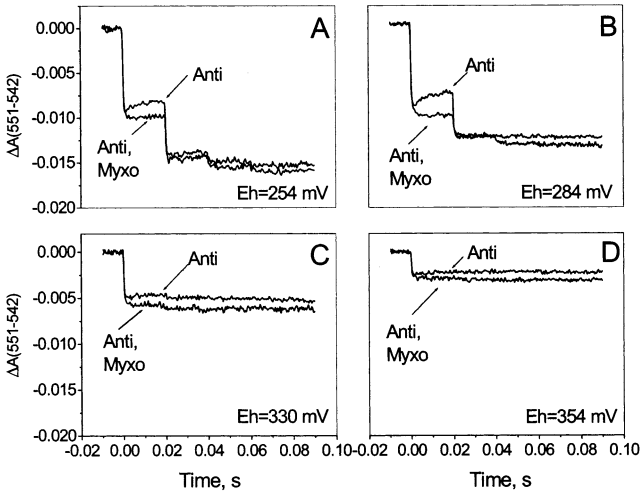

FIGURE 4: Flash-induced kinetics of cytochrome c_{tot} ($=c_1 + c_2$) in the absence and presence of myxothiazol at different redox potentials. Chromatophores from His-tagged *BC17C* cells were suspended in the buffer A (50 mM MOPS, 100 mM KCl, 1mM Fe(III)EDTA, 1 mM NaCN) at pH 7. Additional mediators present were as follows: 60 μM DAD, 50 μM ferrocene, 30 μM *p*-benzoquinone, 2 μM PMS, 2 mM $K_4Fe(CN)_6$. Antimycin A (7 μM) was also present in all samples. The concentrations for CCCP and gramicidin were 3.3 and 40 μM, correspondingly. Traces shown are the average of 16, with 20 s between measurements. E_h was 254 (A), 284 (B), 330 (C), and 354 mV (D).

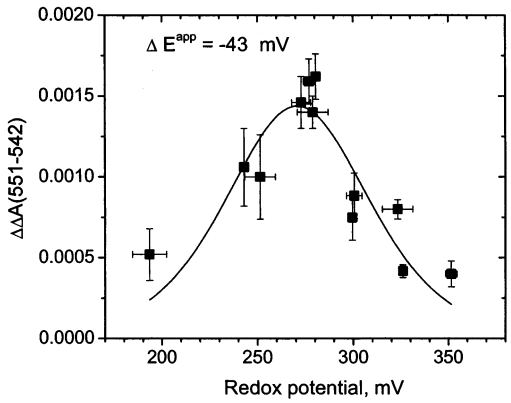

FIGURE 5: Dependence of the increase of amplitude of the cyt c_{tot} induced by the myxothiazol on the redox potential. Each point represents the result of an independent experiment similar to those in Figure 4. Theoretical curve corresponds to the −43 mV shift of midpoint potential of ISP induced by myxothiazol. During calculations it was assumed that c_1 comprises 43% of all cytochrome c_{tot}, as was found from flash-induced kinetics of cytochromes c_1 and c_2 in the presence of antimycin and myxothiazol. Both redox dependencies of ISP and cytochrome c_1 were included in calculations. It was assumed in the fit shown that E_m of ISP and cytochrome c_1 are 290 and 260 mV, respectively. Vertical error bars are the sum of errors due to noise in the subtracted traces; horizontal error bars represent the range of E_h variation during each measurement.

of myxothiazol on the kinetics of cytochromes c_1 and c_2 at $E_h \sim 300$ mV. Kinetics of both cytochromes c_1 and c_2 are changing, but the main effect of myxothiazol on the amplitude of the cyt c_{tot} at this E_h is contributed by changes of cyt c_1 kinetics. The two-exponential fit of the cyt c_1 oxidation kinetics in the presence of antimycin A alone shows components with lifetimes of 0.49 ± 0.06 and 8.2 ± 2.4 ms and amplitudes (31 ± 2)·10^{-4} and (14 ± 1)·10^{-4}, respectively. The two-exponential fit of cyt c_1 kinetics in the presence of both antimycin A and myxothiazol shows rise components with lifetimes of 0.25 ± 0.04 and 4.8 ± 0.9 ms, with amplitudes of (47 ± 8)·10^{-4} and (14 ± 1)·10^{-4}, respectively. The difference in the slower components of the kinetics includes contributions from the oxidation of QH_2 released by RC after flash that are not relevant to the current discussion. Of interest here is the fact that addition of myxothiazol leads to an increase of the fast (<1 ms) component of the cyt c_1 oxidation. Such an increase can be explained by a loss in availability of electrons from ISP^{red} for reduction of cyt c_1 in the presence of myxothiazol (see Discussion for details).

Redox Dependence of the Myxothiazol Effect. Figure 4 shows the flash-induced cyt c_{tot} oxidation in the absence and presence of myxothiazol, measured at different redox potentials. The dependence on E_h of the extra amplitude of cyt c_t oxidation induced by myxothiazol was not a simple Nernst function. The increase is small at E_h < 200 mV and at E_h > 350 mV and is maximal at about 280 mV (Figure 5).

Such nonmonotonic E_h behavior of the myxothiazol effect can be explained by assuming that myxothiazol decreases the midpoint potential of the ISP. By fitting the data shown in Figure 5 (taking account of all equilibria in the high potential chain), one finds that the myxothiazol-induced shift of the midpoint potential of ISP is −43 ± 9 mV. This finding is in good correspondence with a value found recently by Darrouzet et al. (*13*) using equilibrium redox titration of the EPR signal measured at liquid-He temperature.

This small shift explains why such an effect of myxothiazol is seen only over the relatively small region of E_h between 200 and 350 mV. It is only over the range about the midpoint that the small change in E_m on addition of myxothiazol leads to a significant change in the initial concentration of the reduced ISP. At lower redox potentials (E_h < 200 mV), the effect of myxothiazol on the amplitude of c_{tot} is absent because the E_m shift of ISP is not large enough to keep ISP more oxidized before the flash. At higher redox potentials (E_h > 350 mV) the ISP is already mostly oxidized at both E_m values, and no further oxidation can be induced by

myxothiazol; addition of inhibitor should therefore have no effect on the cyt c_{tot} behavior.

Sharp et al. (*15*) found that simple alcohols decreased the midpoint redox potential of ISP measured at low temperature by about 30 mV in *Rb. capsulatus* chromatophore membranes but had no effect on the cytochrome kinetics at room temperature under the conditions tested. Since the published effect of ethanol on E_m of ISP is similar to the effect of myxothiazol found in this paper and since for much of the work, inhibitors in ethanolic solution were used, it was necessary to study the contribution of the alcohol effect to these kinetic phenomena. We found that myxothiazol dissolved in dimethyl sulfoxide had effects similar to those seen when myxothiazol was dissolved in ethanol (not shown). As an additional control, the myxothiazol-induced effect on the oxidation of cyt c_1 was compared with that on addition of alcohol alone. Both these controls indicated that myxothiazol was mainly responsible for the effect observed under the conditions used here. Ethanol alone had a very little effect on the kinetics of cyt c_{tot} at $E_h \approx 280$ mV when added before myxothiazol; no significant effect was seen at 100 mM. Even at 900 mM, the change in amplitude of cyt c_{tot} was <30% of that seen with myxothiazol. This is in agreement with the finding of Sharp et al. (*15*) with respect to kinetics of cyt c_{tot}, but indicates a smaller effect on E_m of ISP than that seen previously. Moreover, further addition of myxothiazol led to the full extra cyt c_{tot} oxidation, indicating that addition of alcohol did not prevent binding of myxothiazol (not shown). Addition of myxothiazol in DMSO gave rise to the maximal effect observed, and subsequent addition of ethanol had no further effect (not shown). Thus, myxothiazol alone is responsible for the observed effects at the concentrations of ethanol used here.

The alcohol and the myxothiazol effects can both be explained by a decrease in E_m of ISP through an interference with the interaction of the ISP with quinone at Q_o binding site, although the mechanism by which they achieve this is likely different (see Discussion).

DISCUSSION

Current Model of ISP Function. The structures of the bc_1 complex indicate that positions occupied by ISP depend on the occupation of the Q_o binding site and on different crystal forms (*7*, *20*−*22*). Because of the constraints of distance on electron-transfer rates in different structures, it was suggested that the ISP functions via anchored movement of the catalytic domain in order to couple oxidation of ubiquinol and reduction of cyt c_1. Thus, in the model shown in Figure 6, ISP can assume two main conformations: near c_1 (C conformation, subscript c) and near cyt *b* (B conformation, subscript b). Our kinetic studies confirm previous reports that myxothiazol or similar class II inhibitors induce a change in E_m of the ISP (*13*, *14*). Since our studies were performed at room temperature, they remove possible ambiguities relating to the measurement of E_m changes through EPR at liquid-He temperatures. The kinetic effects are explained by the fact that, over the range of E_h around the E_m, the lower E_m of ISP in the presence of myxothiazol leads to a lower concentration of its reduced form, which, because the total yield of photo-oxidant was unchanged, increases the flash-induced oxidation of cyt c_{tot} and cyt c_1.

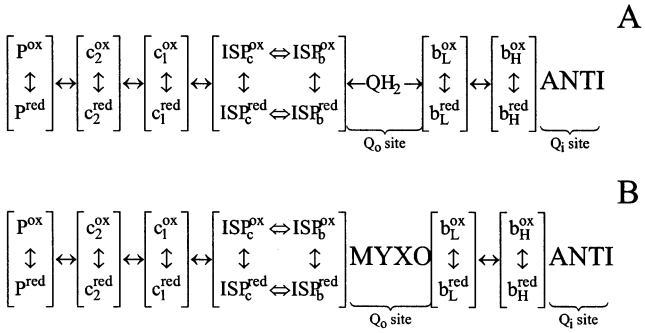

FIGURE 6: Scheme of electron transport in *Rb. sphaeroides* chromatophores in the presence of antimycin A alone (A) and in the presence of both antimycin A and myxothiazol (B). The mobility of ISP in the bc_1 complex is taken into account by introducing two conformations: near c_1 (C conformation, subscript c) and near cyt *b* (B conformation, subscript b). Transitions between different conformations of ISP are indicated by double arrows, ↔.

The E_m change induced by addition of myxothiazol could in principle be due to changes in equilibrium constant for several of the processes involved. From the structures, there are many contacts between the ISP and cyt *b*, including the liganding connection through the H-bond between His-161 of ISP and the site occupant. These are exchanged for a different set of interactions when the ISP is released. There are also other changes in conformation of all three catalytic subunits of the bc_1 complex when the ISP changes its position (*38*). The experimental data provide differential values reflecting all changes in the forces associated with particular changes in state. Each of these interactions has a thermodynamic consequence, and the question arises as to which of these interactions contribute to the E_m change observed.

Simplified Model for Dependence of E_m of ISP on Conformation. To explore in more general terms the thermodynamics involved, we have developed the formal framework below. In the absence of myxothiazol, under conditions where the quinone pool is oxidized, transition of ISP between conformations C (subscript c) and B (subscript b) can be described by the following simplified scheme showing different states of the bc_1 complex (here E_C and E_{B1} are respective midpoint potentials; K_1 and K_2 are respective "binding" equilibrium constants reflecting the conversion from the C state (free) to the B state (bound); Q in brackets indicates that the Q_o site is occupied by ubiquinone):

$$\begin{array}{ccc} ISP_c^{ox} < Q > & \overset{K_1}{\Leftrightarrow} & ISP_b^{ox} < Q > \\ \updownarrow E_C & & \updownarrow E_{B1} \\ ISP_c^{red} < Q > & \overset{K_2}{\Leftrightarrow} & ISP_b^{red} < Q > \end{array} \quad (1)$$

The apparent midpoint potential of ISP, E_Q^{app}, is determined by the Nernst equation:

$$E_h = E_Q^{app} + \frac{RT}{F} \ln \frac{[ISP^{ox}]}{[ISP^{red}]} = E_Q^{app} + \frac{RT}{F} \ln \frac{[ISP_c^{ox}Q] + [ISP_b^{ox}.Q]}{[ISP_c^{red}Q] + [ISP_b^{red}.Q]} \quad (2)$$

where *R*, *T*, and *F* are the gas constant, absolute temperature,

and Faraday constant, respectively, and [ISP^{ox}] ([ISP^{red}]) is the total concentration of oxidized (reduced) ISP.

Expressing the concentration of all forms of ISP in scheme (1) via [ISP_c^{ox}] and [ISP_c^{red}] with use of equilibrium constant K_1 and K_2, we can write from eq 2:

$$E_h = E_C + (RT/F)\ln([ISP_c^{ox}]/[ISP_c^{red}]) \quad (3)$$

where

$$E_C = E_Q^{app} + (RT/F)\ln((1 + K_1)/(1 + K_2)) \quad (4)$$

Equation 4 indicates that the apparent midpoint potential of ISP depends on the binding of the reduced and oxidized forms of ISP with the Q_o site occupied by ubiquinone:

$$E_Q^{app} = E_C + \frac{RT}{F}\ln((1 + K_2)/(1 + K_1)) \quad (5)$$

This equation indicates that the midpoint potential of ISP, E_Q^{app}, will be equal to the midpoint potential of ISP in C conformation, E_C, only when $(1 + K_2) \approx (1 + K_1)$. This can be observed when both binding constants are small ($K_1 < 1$, $K_2 < 1$), or equal. In other words, the midpoint potential of ISP will be modified by occupants of the Q_o binding site only if they increase binding of ISP in the B conformation, with different affinities for oxidized and reduced forms.

In the presence of myxothiazol or other inhibitors at the Q_o binding site, the above scheme can be modified as follows:

$$\begin{array}{ccc} ISP_c^{ox} < Inh > & \overset{K_3}{\Leftrightarrow} & ISP_b^{ox} < Inh > \\ \updownarrow E_C & & \updownarrow E_{B2} \\ ISP_c^{red} < Inh > & \overset{K_4}{\Leftrightarrow} & ISP_b^{red} < Inh > \end{array} \quad (6)$$

Here Inh stands for inhibitor.

In full analogy with the case when Q_o site was occupied by ubiquinone (eq 5), we can write the observed midpoint potential of ISP for the case when Q_o site is occupied by the inhibitor:

$$E_{Inh}^{app} = E_C + (RT/F)\ln((1 + K_4)/(1 + K_3)) \quad (7)$$

The change in apparent midpoint potential of ISP induced by an inhibitor can be found as the difference of eqs 7 and 5:

$$\Delta E_{Inh}^{app} = E_{Inh}^{app} - E_Q^{app} = \frac{RT}{F}\ln\frac{(1 + K_1)(1 + K_4)}{(1 + K_2)(1 + K_3)} \quad (8)$$

This expression shows that the observed shift of midpoint potential of ISP can be due to the differences in binding of reduced and oxidized ISP with the Q_o binding site occupied by Q or (and) by inhibitor.

The formalism outlined above is somewhat different from the classical approach originally developed by Clark (*34*) for redox changes associated with ligand binding in soluble systems. Our treatment is appropriate for the particular case of tethered diffusion, which makes it possible to treat the ISP system as involving a set of first-order processes in which the binding constants are dimensionless ratios. This ignores the second-order effects associated with concentration dependence of the inhibitors and quinone. In principle, the simplification allows for exact solution only for a defined set of concentrations. In practice, in the experiments reported here, the quinone concentration was always set by the composition of the chromatophore membrane (30−60-fold ratio of quinone to bc_1 complex) and the high E_h, and the inhibitors were used at saturating concentration.

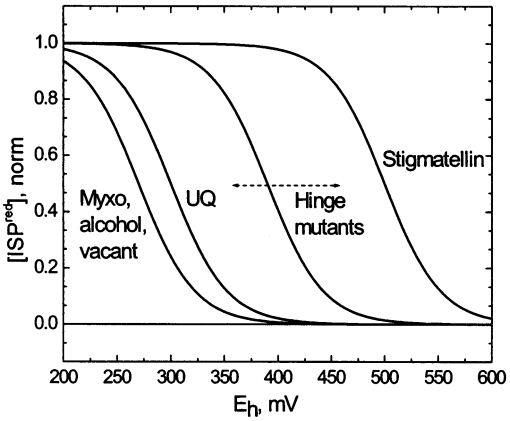

FIGURE 7: Effect of the occupants of Q_o binding site on the midpoint potential of ISP calculated from eq 8. In the case of a vacant Q_o site, we assumed that both binding constants in the equation are less than 1 ($K_1 < 1$, $K_2 < 1$, $K_3 = 0$, $K_4 = 0$). Effectively, this is the same as the case in the presence of class II (Q_o-I) inhibitors (myxothiazol, MOA−stilbene), or alcohol. Similarly, this case should correspond to the isolated ISP. In the case when Q_o binding site is occupied by quinone, we assumed in eq 8 that $K_1 < 1$, $K_2 > 1$, $K_3 = 0$, and $K_4 = 0$. Similarly, when the Q_o binding site is occupied by a class I inhibitor (UHDBT or stigmatellin), we assumed in eq 8 that $K_1 < 1$, $K_2 > 1$, $K_3 = 0$, and $K_4 \gg 1$.

A more general scheme is given in an appendix, with equivalences relating the terms used above to the more cumbersome expressions developed fully there. The model developed is a general phenomenological model that includes both conformational movement of the ISP and the influence of the occupation of Q_o site on ISP potential. The interpretation of this model is dependent on the particular occupant of Q_o site, but the model itself does not depend on the nature of the forces involved. The values for equilibrium constants (or the $\Delta G°$ values) can be thought of as the product (or sum for $\Delta G°$ values) of all contributions to the transitions between states involved. The general solution given by eq 8 and the formalism summarized in the scheme in the appendix (Figure 8) are not dependent on any assumptions about the underlying mechanism other than the specification of transitions between the states shown. Thus, it has wide application as a general model for interactions of ISP with occupants of Q_o site.

Effect of Myxothiazol and Other Inhibitors. Equation 8 can be simplified further in the case of myxothiazol binding. One can assume, as a first approximation, that in the presence of myxothiazol, the binding equilibrium constants (affinities) of oxidized and reduced ISP for the B conformation are small ($K_4 \ll 1$, $K_3 \ll 1$). This is justified by the structures of the bc_1 complex, which indicate that ISP found in the B position in the native complex had moved to the C conformation in the presence of myxothiazol (*20*, *32*). In this case, eq 8 takes the form

$$\Delta E_{myxo}^{app} = (RT/F)\ln((1 + K_1)/(1 + K_2)) \quad (9)$$

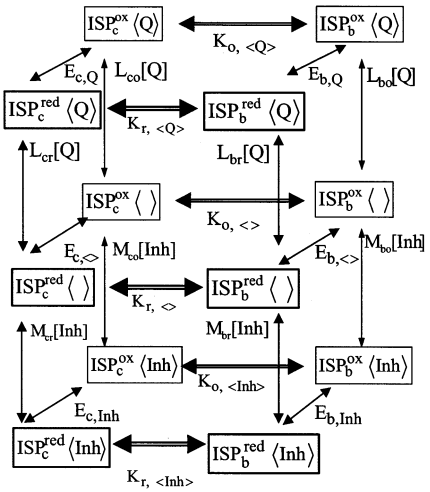

FIGURE 8: Scheme of ISP redox and conformational transitions as function of occupation of the Q_o site (shown here by brackets, ⟨⟩). Here vertical transitions reflect changes in occupation of Q_o site, horizontal transitions reflect changes in the conformation of ISP, and diagonal transitions reflect changes of the redox state of ISP. Both vertical and diagonal transitions are second-order reactions, while horizontal transitions are first-order reactions. Transitions of ISP between B and C conformations are characterized here by equilibrium constant K, the lower index of which indicates both the redox state of ISP (o or r for oxidized or reduced forms, respectively) and the occupation of the Q_o binding site (⟨⟩, ⟨*Q*⟩, and ⟨*Inh*⟩ for vacant, occupied by ubiquinone, and occupied by inhibitor, respectively). Binding of ubiquinone is characterized by equilibrium constants *L*, the lower index of which indicates the conformation (B or C) and state of oxidation (o or r for oxidized or reduced forms, respectively) of ISP. Binding of inhibitor is characterized by equilibrium constants *M*, the lower index of which indicates the conformation (B or C) and state of oxidation (o or r for oxidized or reduced forms, respectively) of ISP. The redox potential of ISP is characterized by midpoint potential *E*, the lower index of which indicates both the conformation of ISP (index B or C) and the occupation of the Q_o binding site (⟨⟩, ⟨*Q*⟩, and ⟨*Inh*⟩ for unoccupied, occupied by ubiquinone, and occupied by inhibitor, respectively).

If we further assume, as seems likely, that in the absence of inhibitor, the binding constant for the oxidized form of ISP with quinone is small ($K_1 \ll 1$), then the apparent shift of the midpoint potential of ISP will be a function only of the binding constant of the reduced of ISP at the Q_o binding site, reflecting the interaction with quinone:

$$\Delta E_{myxo}^{app} = -60 \log(K_2 + 1) \qquad (10)$$

This simplified equation is useful for estimation of a minimal value for the binding constant of the reduced form of ISP with quinone at the Q_o site.

From Figure 5, $\Delta E_{myxo}^{app} \approx -43$ mV giving

$$K_2 \approx 5.2-1 = 4.2 \qquad (11)$$

Thus, the binding constant of the reduced form of the ISP with quinone occupying the Q_o site is ≥ 4.

A negative shift in the E_m of ISP of about 30−50 mV, induced by MOA−stilbene (14), is close to that of myxothiazol found here. A similar value from titration was also briefly reported by Darrouzet et al. (*13*) for the change induced by myxothiazol. At first sight, it looks as if all class II (Q_o-I) inhibitors shift the E_m of ISP in the negative direction. In view of the evidence from the detailed molecular structures that there are no interactions of ISP with the inhibitors, this is anomalous and would require an explanation in terms of differential interaction with the protein. However, the obverse description provides a more mechanistically relevant insight into the nature of these shifts; − all occupants of the Q_o site that provide a H-bonding ligand to the reduced ISP shift the E_m in a positive direction compared to the unliganded form (Figure 7). From the analysis above, the effect seen on addition of myxothiazol can be explained simply in terms of displacement of the quinone. Thus, the effect of class II (Q_o-I) inhibitors is mostly due to the removal of the interaction of the reduced form of ISP with ubiquinone occupying the binding site.

Effect of Stigmatellin and Other Class I (Q_o-II and Q_o-III) Inhibitors. Equation 8 can also be used for the estimation of binding constants of ISP in the B conformation for class I inhibitors such as stigmatellin. Indeed, in contrast to class II inhibitors, the binding of class I inhibitors at Q_o site leads to strong binding of the reduced form of ISP in the B conformation ($K_4 \gg 1$). Assuming as before that binding of the oxidized form of ISP to Q_o binding site occupied by quinone or inhibitor is weak ($K_1 < 1$, $K_3 < 1$), we have

$$\Delta E_{Class\ I}^{app} = E_{inh}^{app} - E_{Q}^{app} \approx \frac{RT}{F} \ln \frac{(1 + K_4)}{(1 + K_2)} \qquad (12)$$

Thus, when the Q_o binding site is occupied by class I inhibitors, the observed shift is determined by the ratio of the binding constants of the reduced form of ISP with the Q_o binding site occupied by inhibitor (K_4) and ubiquinone (K_2).

Using the estimation for ($K_2 + 1$) given by eq 10, we can write

$$\Delta E_{Class\ I}^{app} \approx 60 \log(K_4) + \Delta E_{myxo}^{app} = 60 \log(K_4) - 43 \text{ mV} \qquad (13)$$

or

$$60 \log(K_4) \approx \Delta E_{Class\ I}^{app} + 43 \text{ mV} \qquad (14)$$

In the case of stigmatellin, the measured shift of the E_m for ISP is about 200 mV. This means that binding constant for ISP in the reduced form when stigmatellin is occupying Q_o binding site is about 10^4.

Effects of Specific Mutation of the Hinge Region of ISP on the Binding Constant. Darrouzet et al. (*13*) reported redox titrations of the EPR signal of the [2Fe−2S] cluster in wild type and mutant strains in which the length of the linker span connecting the mobile extrinsic domain to its anchoring N-terminus was varied by insertion or deletion of residues. They found that several mutations in the hinge region led to an increase in E_m of the ISP. However, this increase of E_m disappeared in the presence of myxothiazol. This effect of myxothiazol opens the possibility that new insights into the mechanism of the change in E_m induced by mutation might be gained by re-interpretation in the light of our analysis above. If the effect of myxothiazol in decreasing the midpoint potential of ISP occurs by the mechanism we have suggested—by disrupting the interaction of the ISP with ubiquinone at the Q_o binding site—then the increase in E_m of ISP in these mutants can be explained simply by an increase of the

binding constants for the reduced form of ISP with ubiquinone at the binding site. In this case, the effect of mutation can be described by eq 5:

$$E_Q^{app} = E_C + \frac{RT}{F}\frac{(1+K_2)}{(1+K_1)} \approx E_C + 60 \log K_2 \quad (15)$$

The measured shift of ISP midpoint potential for the 6Pro mutant is about 230 mV (*13*), indicating that binding constant K_2 in this case is $6.8 \cdot 10^3$, more than a 1000-fold increase in comparison to $K_2 = 4.2$ for the wild type, determined here. Other strains with lengthened linkers showed substantial, though smaller, increases in K_2.

Effects of Alcohols on the E_m of the ISP. Our model also provides a natural explanation for the results of Sharp et al. (*15*), who found that ethanol decreases the midpoint redox potential of ISP by about 30 mV in *Rb. capsulatus* chromatophores. The similarity between the value for the E_m change induced by alcohol and that induced by myxothiazol (this work) and MOA stilbene (*14*) and the complete absence of any effect of alcohol in the presence of myxothiazol (this work) indicate that the main target of alcohol is not binding to the reduced form of ISP as previously suggested. The simplest explanation would be that alcohols interfere with the differential binding of the reduced form of ISP with quinone. Since the −OH group of an alcohol provides a potential H-bond donor, we suggest that the alcohols compete with the reduced ISP as H-bond donors to the quinone. By forming a H-bond with quinone, the alcohols inhibit the formation of H-bond with ISP, preventing the interaction that raises the E_m. The alternative, that alcohols act as H-bond donors to the oxidized ISP, seems less probable because an effect of alcohols on the rate of electron transfer, expected if one of the substrates for the ES complex was competitively bound, was not observed. From our own results, the effect of alcohols on the E_m value of ISP at room temperature are less than those observed by Sharp et al. (*15*) when measuring the E_m at liquid-He temperature. A possible explanation might be found in the phase separation, which would give rise to a higher local concentration of alcohol on freezing.

What Forces Contribute to the Change in E_m Induced by Myxothiazol? Information about the nature of the forces contributing to the differential changes comes from several lines of evidence. The structural data and recent ESEEM experiments (*33*) clearly point to the H-bonding interaction as an important factor stabilizing the liganding configuration. The change on addition of myxothiazol involves loss of the H-bond, so it is clearly necessary to include that in discussion. Since the change in each case is measured through the E_m of ISP, it must reflect specifically the interaction energy of the ISP.

The data of Darrouzet et al. (*13*, *16*) for ISP mutants are of particular interest in allowing an estimation of changes in the free energies for some transitions. For example, all mutant ISPs showed the same value of E_m as the wild type in the presence of myxothiazol. We can therefore conclude that the mutations had no effect on the E_m except those specific to the interactions in the absence of myxothiazol. Similarly, except in the case of the 6Pro strain, the E_m was the same in the presence of stigmatellin. We can therefore conclude that, except in the 6Pro strain, the mutations had no additional effect leading to a change in binding free energy for the ISP in the liganding configuration. In the case of the 6Pro strain, the additional term was 30 mV.

One can extrapolate from the data the following conclusions: (i) Whatever the effect of myxothiazol, it eliminates all interactions leading to the higher E_m in all strains. Since myxothiazol is bound at the distal end of the Q_o pocket, its main effect is that of displacement of the quinone, and therefore loss of specific interactions between quinone and ISP^{red}. The structures show no interaction between myxothiazol itself and ISP^{red}. (ii) The effects of mutation on E_m are seen only in the absence of myxothiazol and must therefore reflect the configuration in which the ISP^{red} is interacting with the Q_o site and liganding the occupant, presumably quinone in the native complex. (iii) It is reasonable to suppose that the configuration of the interface between cyt b and ISP^{red} is similar when quinone or stigmatellin occupy the Q_o site. Mutations did not prevent the normal interaction of ISP^{red} with stigmatellin and, except for the effect in 6Pro strain, did not introduce any additional free-energy terms affecting the E_m. (iv) In the +2 Ala strain, a normal forward electron transfer for one turnover of the site, presumably through a normal ES complex, was seen when the ISP was initially oxidized (*16*). The binding interface between the cluster domain of ISP and cyt *b* is therefore not likely to have changed much in this or, by extrapolation, the other mutant strains.

From points iii and iv, it seems reasonable to conclude that the main change in the mutant strains is due to a change in the H-bond between His-161 and the occupant.

This simple hypothesis accounts economically for the data and is well supported by the structures available. We assume that when ISP is in the B conformation, it can interact through H-bond formation with ubiquinone (for ISP^{red}) or with ubiquinol (for ISP^{ox}) located at the Q_o binding site, as exemplified by the H-bond of stigmatellin with ISP found in crystals with stigmatellin at Q_o binding site (*7*, *24*, *32*; reviewed in ref *1*). Experimental support for such a H-bonded complex with quinone has come from measurement of the orientation of the bridging histidine by using 1D and 2D ESEEM (*33*). It was found that the complex between quinone and ISP^{red} was similar to that seen between stigmatellin and ISP^{red}. In both cases, the orientation of one of the histidine ligands, measured through hyperfine and quadrupole couplings with the $^{14}N_\delta$, was different from that in the presence of myxothiazol, when the two histidine ligands were more nearly equivalent. From the similarities with the stigmatellin case, we suggest that this buried H-bond contributes the major factor leading to stronger binding of the reduced form of ISP^{red} in the B conformation.

Relative Affinities of the Q_o Site for Quinone and Quinol. The one set of data from Darrouzet et al. (*13*) that may not be accounted for by our minimal hypothesis is that the $g_x = 1.8$ signal titrates with a similar $E_{m,7}$ in the 6Pro mutant (~80 mV) and the wild type (~90 mV), both close to the E_m of the quinone pool (~90 mV). Interpretation depends on the mechanistic explanation. It was originally suggested by Matsuura et al. (*37*) that the Q_o site with ISP^{red} binds the quinone (Q) form and the quinol (QH_2) form equally. Following this explanation, one would have to say that in the mutant strains, the same applies, as suggested by Darrouzet et al. (*13*). In this case, the data are not in conflict with our simple hypothesis. However, in wild-type such an

explanation lacks a mechanistic base because the CW-EPR spectrum with QH_2 has no prominent g_x feature, and a H-bond between ISP^{red} and QH_2 of the same strength as that with Q seems unlikely. Alternative mechanisms have been proposed in which the binding of QH_2 does not involve ISP^{red} (*32*). The spectroscopic information favors this latter type of explanation; in addition, Glu-272 offers a possible ligand for QH_2, but not for Q (*24*), to provide the necessary thermodynamic term. If this scenario applied to the 6Pro strain and the ISP^{red} preferentially bound Q but did not bind QH_2, one might expect from our simple hypothesis a shift of the titration curve to lower values in the strains with tighter ligation, which is not seen. However, in the 6Pro strain, the CW-EPR spectrum in the presence of QH_2 showed a sharp g_x feature (*13*), which might indicate a liganding configuration for ISP^{red} under these conditions not found in the wild type. This need not necessarily involve QH_2, since the structures show several other potential H-bonding partners (*38*). An additional ligand would provide a mechanistic basis for the hypothesis of Darrouzet et al. (*13*) and would not be inconsistent with our simple hypothesis. However, until this point is resolved, the minimal hypothesis must be treated as tentative.

Mechanistic Implications. Given the complexity of the system, one could make an infinite set of hypotheses to explain the data. The simplest of these is the one we have preferred, since it accounts for most of the data without supplementary ad hoc assumptions. It is noteworthy in this context that all the changes in E_m values with inhibitors, or quinone in mutant strains (Figure 7), fall in the range between the value in the presence of myxothiazol ($E_m \sim 265$ mV) and that in the presence of stigmatellin ($E_m \sim 500$ mV). Since the nature of the binding effect we have postulated through the H-bond is the same in each case (ring $>C{=}O\cdots HN_\delta-$ histidine-161), it is pertinent to ask what structural difference might give rise to the different values for the binding constant for the mutant strains in the absence of inhibitor. As noted above, the simplest hypothesis is that a major contribution comes from the H-bond between ISP His-161 and the Q_o site occupant. The maximal value for binding free-energy with stigmatellin is in the range expected for H-bonds in a nonpolar environment (20−25 kJ mol^{-1}), consistent with the buried anhydrous location shown by the structures (*35*). It seems unlikely, since in all mutant strains the g_x lines in the absence of inhibitor were similar to that of wild type (*13*), that gross differences in location or environment can account for the large differences seen in E_m. We can reasonably conclude that in all strains the EPR signal indicates a H-bond with quinone. In this context, the fact that increased length of the linker led to increased binding suggests an interesting possibility. Structures of the bc_1 complex show that the linker region is fully extended in the presence of stigmatellin, but is in a helical configuration in the presence of myxothiazol. It seems possible that the linker region, and possibly other features modulating the interaction, have been designed by evolution so as to provide a less than optimal H-bond configuration for interaction with quinone (or with quinol in the ES-complex). With the same protein conformation, the larger ring of stigmatellin (6.06 Å between liganded O-atoms compared to 5.36 Å in quinone) might allow a shorter H-bond length, giving a binding constant at the high end of the range. We suggest that in the strains with a longer or more flexible hinge, the ISP can find a configuration that allows a tighter binding than in the native complex. In the mutant strains, the degree of inhibition was scaled with the increase in E_m (*16*), indicating that the ability of the ISP to participate in the movement required for rapid turnover was impaired by the increased binding constant. Since the binding constant is a ratio of rate constants for association and dissociation, and the association will depend mainly on collisional frequency, it seems likely that the slowed rate reflected predominantly a slowed dissociation. The relatively weak binding seen in the native complex with quinone (this work), or of ISP^{ox} with ubiquinol (*7*, *24*, *32*, *36*), might therefore indicate that the natural structure has evolved so as to lower the affinity. We might think of the conformational strain involved as a spring-loading of the structure for states involving the interaction of the ISP with the native quinone or quinol, so as to favor rapid leaving times for intermediate states. In the context of the ES complex, the spring loading would have two effects: (i) it would minimize the binding energy, and hence the trough in the reaction-energy profile; (ii) it would facilitate rapid dissociation of ISP^{red} after electron transfer from QH_2, and hence rapid redox shuttling in the high potential chain (*32*, *36*).

CONCLUSIONS

The kinetics of flash-induced oxidation and reduction of cytochromes c_{tot}, c_1, and c_2 in *Rb. sphaeroides* chromatophores were followed at different myxothiazol concentrations and at different redox potentials. Addition of myxothiazol to chromatophores at $E_h \sim 300$ mV led to an increase in amplitude of the flash-induced oxidation of cyt c_1, due to a decreased ability of ISP to donate an electron to cyt c_1. This increase of flash-induced oxidation of cyt c_1 is absent at E_h below 200 mV and at E_h above 350 mV, indicating that myxothiazol induces the oxidation of ISP. To explain this effect of myxothiazol, a simple model is used to connect binding of oxidized and reduced forms of ISP in the B conformation (near b_L heme) with changes of apparent midpoint potential of ISP. Binding of myxothiazol at the Q_o site leads to the release of ISP from the B conformation. As a consequence, it eliminates any differences in binding of the reduced and oxidized forms of the ISP with the quinone occupying Q_o site. It is estimated that the binding constant of the reduced form of ISP in the B conformation, when the Q_o binding site is occupied by quinone, is about 4. We identify the H-bond between the liganding histidine of ISP and the Q_o site occupant as a major contributor to the change in midpoint potential and discuss previous observation in the light of this minimal hypothesis. The relatively weak binding seen in the native complex between ISP^{red} and quinone or ISP^{ox} and quinol suggests that the natural structure of ISP favors rapid leaving times for intermediate states, and therefore rapid turnover.

APPENDIX 1. ANALYSIS OF GENERAL SCHEME DESCRIBING CONFORMATIONAL TRANSITIONS OF ISP FOR DIFFERENT OCCUPATION OF Q_O BINDING SITE

The apparent midpoint potential of ISP, E^{app}, is determined by the Nernst equation

$$E_h = E^{app} + \frac{RT}{F} \ln \frac{[ISP^{ox}]}{[ISP^{red}]} \quad (A1)$$

where R, T, F are the gas constant, absolute temperature, and Faraday constant, respectively, and $[ISP^{ox}]$ ($[ISP^{red}]$) is the total concentration of oxidized (reduced) ISP.

Similarly, for ISP in the C conformation with a vacant Q_o site:

$$E_h = E_{c,\langle\rangle} + \frac{RT}{F} \ln \frac{[ISP_c^{ox}\langle\rangle]}{[ISP_c^{red}\langle\rangle]} \quad (A2)$$

where $E_{c,\langle\rangle}$ is the midpoint potential for ISP in C conformation with vacant Q_o binding site.

The ratio of oxidized and reduced forms of ISP determined from the Figure 8 is as follows:

$$\frac{[ISP^{ox}]}{[ISP^{red}]} = ([ISP_c^{ox}\langle Q\rangle] + [ISP_c^{ox}\langle\rangle] + [ISP_c^{ox}\langle Inh\rangle] + [ISP_b^{ox}\langle Q\rangle] + [ISP_b^{ox}\langle\rangle] + [ISP_b^{ox}\langle Inh\rangle])/([ISP_c^{red}\langle Q\rangle] + [ISP_c^{red}\langle\rangle] + [ISP_c^{red}\langle Inh\rangle] + [ISP_b^{red}\langle Q\rangle] + [ISP_b^{red}\langle\rangle] + [ISP_b^{red}\langle Inh\rangle]) \quad (A3)$$

Expressing the concentration of all forms of ISP in Figure 8 via $[ISP_c^{ox}\langle\rangle]$ and $[ISP_c^{red}\langle\rangle]$ with use of respective equilibrium constants, one can write

$$\frac{[ISP^{ox}]}{[ISP^{red}]} = [ISP_c^{ox}\langle\rangle](1 + K_{o,\langle\rangle} + L_{co}[Q](1 + K_{o,\langle Q\rangle}) + M_{co}[Inh](1 + K_{o,\langle Inh\rangle}))/[ISP_c^{red}\langle\rangle](1 + K_{r,\langle\rangle} + L_{cr}[Q](1 + K_{r,\langle Q\rangle}) + M_{cr}[Inh](1 + K_{r,\langle Inh\rangle})) \quad (A4)$$

Taking logarithms of both sides of this equation, and replacing ratio of concentrations of ISP according to eqs A1 and A2, one can find that

$$E^{app} = E_{c,\langle\rangle} + (RT/F) \ln \left(\frac{1 + K_{r,\langle\rangle} + L_{cr}[Q](1 + K_{r,\langle Q\rangle}) + M_{cr}[Inh](1 + K_{r,\langle Inh\rangle})}{1 + K_{o,\langle\rangle} + L_{co}[Q](1 + K_{o,\langle Q\rangle}) + M_{co}[Inh](1 + K_{o,\langle Inh\rangle})} \right) \quad (A5)$$

This equation describes, in general terms, the effect of occupation of Q_o binding site and conformational transitions of ISP between B and C conformations on the apparent midpoint potential of ISP.

In the absence of inhibitor ($[Inh] = 0$), eq A5 takes the form

$$E^{app} = E_{c,\langle\rangle} + (RT/F) \ln \left(\frac{1 + K_{r,\langle\rangle} + L_{cr}[Q](1 + K_{r,\langle Q\rangle})}{1 + K_{o,\langle\rangle} + L_{co}[Q](1 + K_{o,\langle Q\rangle})} \right) \quad (A6)$$

Thus, in the absence of inhibitors, the apparent E_m of ISP depends on quinone concentration and on the respective equilibrium constants of quinone binding at Q_o site, as well as on equilibrium constants of transition of oxidized and reduced forms of ISP between C and B conformations.

For high quinone concentration ($L_{cr}[Q](1 + K_{r,\langle Q\rangle}) \gg 1 + K_{r,\langle\rangle}$, $L_{co}[Q](1 + K_{o,\langle Q\rangle}) \gg 1 + K_{o,\langle\rangle}$), the apparent E_m of ISP does not depend on quinone concentration anymore:

$$E^{app} = E_Q^{app} = E_{c,\langle\rangle} + (RT/F) \ln \left(\frac{L_{cr}(1 + K_{r,\langle Q\rangle})}{L_{co}(1 + K_{o,\langle Q\rangle})} \right) \quad (A7)$$

We can assume that when ISP is in the C conformation the binding of quinone is independent of the redox state of ISP, i.e., $L_{cr} = L_{co}$.

Thus

$$E^{app} = E_Q^{app} = E_{c,\langle\rangle} + (RT/F) \ln \left(\frac{1 + K_{r,\langle Q\rangle}}{1 + K_{o,\langle Q\rangle}} \right) \quad (A8)$$

This expression is identical to the eq 5 of the main text with

$$K_1 \equiv K_{o,\langle Q\rangle} \quad (A9)$$

$$K_2 \equiv K_{r,\langle Q\rangle} \quad (A10)$$

In the presence of a specific inhibitor, ($M_{cr}[Inh](1 + K_{r,\langle Inh\rangle}) \gg 1 + K_{r,\langle\rangle} + L_{cr}[Q](1 + K_{r,\langle Q\rangle})$, and

$$M_{co}[Inh](1 + K_{o,\langle Inh\rangle}) \gg 1 + K_{o,\langle\rangle} + L_{co}[Q](1 + K_{o,\langle Q\rangle}))$$

Then, eq A5 takes the form

$$E^{app} = E_{Inh}^{app} = E_{c,\langle\rangle} + (RT/F) \ln \left(\frac{M_{cr}(1 + K_{r,\langle Inh\rangle})}{M_{co}(1 + K_{o,\langle Inh\rangle})} \right) \quad (A11)$$

Again, we can assume that when ISP is in the C conformation the binding of inhibitor is independent of the redox state of ISP:

$$M_{cr} = M_{co} \quad (A12)$$

Thus

$$E^{app} = E_{Inh}^{app} = E_{c,\langle\rangle} + (RT/F) \ln \left(\frac{1 + K_{r,\langle Inh\rangle}}{1 + K_{o,\langle Inh\rangle}} \right) \quad (A13)$$

This expression is identical to the eq 7 of the main text with

$$K_3 \equiv K_{o,\langle Inh\rangle} \quad (A14)$$

$$K_4 \equiv K_{r,\langle Inh\rangle} \quad (A15)$$

The difference of apparent midpoint potentials given by eqs 8A and 13A, is as follows:

$$\Delta E^{app} = E_{Inh}^{app} - E_Q^{app} = (RT/F) \ln \left(\frac{1 + K_{o,\langle Q\rangle}}{1 + K_{r,\langle Q\rangle}} \right) \left(\frac{1 + K_{r,\langle Inh\rangle}}{1 + K_{o,\langle Inh\rangle}} \right) \quad (A16)$$

This equation is identical to eq 8 of the main text, with the equivalences for K terms already noted above.

REFERENCES

1. Berry, E. A., Guergova-Kuras, M., Huang, L. S., and Crofts, A. R. (2000) *Annu. Rev. Biochem. 69*, 1005−1075.

2. Mitchell, P. (1976) *J. Theor. Biol. 62*, 327−367.
3. Crofts, A. R., Meinhardt, S. W., Jones, K. R., and Snozzi, M. (1983) *Biochim. Biophys. Acta 723*, 202−218.
4. von Jagow, G., and Link, T. A. (1986) *Methods Enzymol. 126*, 253−271.
5. Bowyer, J. R., Dutton, P. L., Prince, R. C., and Crofts, A. R. (1980) *Biochim. Biophys. Acta 592*, 445−460.
6. Meinhardt, S. W., and Crofts, A. R. (1982a) *FEBS Lett. 149*, 217−222.
7. Crofts, A. R., Barquera, B., Gennis, R. B., Kuras, R., Guergova-Kuras, M., and Berry, E. A. (1999) *Biochemistry 38*, 15807−15826.
8. Zhang, L., Tai, C. H., Yu, L., and Yu, C. A. (2000) *J. Biol. Chem. 275*, 7656−7661.
9. Tsai, A. L., Kauten, R., and Palmer, G. (1985) *Biochim. Biophys. Acta 806*, 418−426.
10. Meinhardt, S. W., and Crofts, A. R. (1982b) *FEBS Lett. 149*, 223−227.
11. Meinhardt, S. W. (1984) Ph.D. Thesis, University of Illinois at Urbana-Champaign, Urbana-Champaign, IL.
12. Brandt, U., and von Jagow G. (1991) *Eur. J. Biochem. 195*, 163−170.
13. Darrouzet, E., Valkova-Valchanova, M., and Daldal, F. (2002) *J. Biol. Chem. 277*, 3464−3470.
14. Sharp, R. E., Gibney, B. R., Palmitessa, A., White, J. L., Dixon, J. A., Moser, C. C., Daldal, F., and Dutton, P. L. (1999) *Biochemistry 38*, 14973−14980.
15. Sharp, R. E., Palmitessa, A., Gibney, B. R., Moser, C. C., Daldal, F., and Dutton, P. L. (1998) *FEBS Lett. 431*, 423−426.
16. Darrouzet, E., Valkova-Valchanova, M., Moser, C. C., Dutton, P. L., and Daldal, F. (2000) *Proc. Natl. Acad. Sci. U.S.A. 97*, 4567−4572.
17. Von Jagow, G., Ljungdahl, P. O., Graft. P, Ohnishi, T., and Trumpower, B. L. (1984) *J. Biol. Chem. 259*, 6318−6326.
18. Brandt, U., Haase, U., Schagger, H.. and von Jagow, G. (1991) *J. Biol. Chem. 266*, 19958−19964.
19. Xia, D., Yu, C. A., Kim, H., Xia, J. Z., Kachurin, A. M., Zhang, L., Yu, L., and Deisenhofer, J. (1997) *Science 277*, 60−66.
20. Kim, H., Xia, D., Yu, C. A., Xia, J. Z., Kachurin, A. M., Zhang, L., Yu, L., and Deisenhofer, J. (1998) *Proc. Natl. Acad. Sci. U.S.A.* 95, 8026−8033.
21. Zhang, Z., Huang, L., Shulmeister, V. M., Chi, Y. I., Kim, K. K., Hung, L. W., Crofts, A. R., Berry, E. A., and Kim, S. H. (1998) *Nature 392*, 677−684.
22. Iwata, S., Lee, J. W., Okada, K., Lee, J. K., Iwata, M., Rasmussen, B., Link, T. A., Ramaswamy, S., and Jap, B. K. (1998) *Science, 281*, 64−71.
23. Ding, H., Moser, C. C., Robertson, D. E., Tokito, M., Daldal, F., and Dutton, P. L. (1995) *Biochemistry 34*, 15979−15996.
24. Crofts, A. R., Hong, S., Ugulava, N., Barquera, B., Gennis, R., Guergova-Kuras, M., and Berry, E. A. (1999) *Proc. Natl. Acad. Sci. U.S.A. 96*, 10021−10026.
25. Brandner, J. P., McEwan, A. G., Kaplan, S., and Donohue, T. J. (1989) *J. Bacteriol. 171*, 360−368.
26. Guergova-Kuras, M., Salcedo-Hernandez, R., Bechmann, G., Kuras, R., Gennis, R. B., and Crofts, A. R. (1999) *Protein Expression Purif. 15*, 370−380.
27. Drachev, L. A., Kaurov, B. S., Mamedov, M. D., Mulkidjanian, A. Ja., Semenov, A. Ju., Shinkarev, V. P., Skulachev, V. P., and Verkhovsky, M. I. (1989) *Biochim. Biophys. Acta 973*, 189−197.
28. Bowyer, J. R., Meinhardt, S. W., Tierney, G. V., and Crofts, A. R. (1981) *Biochim. Biophys. Acta 635*, 167−186.
29. Dutton, P. L., Petty, K. M., Bonner, S., and Morse, S. D. (1975) *Biochim. Biophys. Acta 387*, 536−556.
30. Shinkarev, V. P., Dracheva, S. M., and Drachev, A. L. (1990) *FEBS Lett. 261*, 11−13.
31. Shinkarev, V. P., Wraight, C. A., and Crofts, A. R. (2001) *Biochemistry, 40*, 12584−12590
32. Crofts, A. R., Hong, S., Zhang, Z., and Berry, E. A. (1999) *Biochemistry 38*, 15827−15839.
33. Samoilova, R. I., Kolling, D., Uzawa, T., Iwasaki, T., Crofts, A. R., and Dikanov, S. A. (2002) *J. Biol. Chem. 277*, 4605−4608.
34. Clark, W. M. (1972) *Oxidation-Reduction Potentials of Organic Systems*, Robert E. Krieger Publishing Company, Huntington, NY.
35. Hunte, C., Koepke, J., Lange, C., Roβmanith, T., and Michel, H. (2000) *Structure 8*, 669−684.
36. Hong, S. J., Ugulava, N., Guergova-Kuras, M., and Crofts, A. R. (1999) *J. Biol. Chem. 274*, 33931−33944.
37. Matsuura, K., Bowyer, J. R., Onhishi, T., and Dutton, P. L. (1983) *J. Biol. Chem. 258*, 1571−1579.
38. Crofts, A. R., Guergova-Kuras, M., Huang, L.-S., Kuras, R., Zhang, Z. and Berry, E. A. (1999) *Biochemistry 38*, 15791−15806.
39. Crofts, A. R., Guergova-Kuras, M., Kuras, R., Ugulava, N., Li, J. and Hong, S. (2000) *Biochim. Biophys. Acta 1459*, 456−466. <<

BI026198C